

V. Vignal, D. Kempf

ICB, UMR 5209 CNRS-Université de Bourgogne, BP 47870, 21078 Dijon Cedex, France

INFLUENCE OF HETEROGENEOUS PLASTIC STRAIN FIELDS ON THE CORROSION SUSCEPTIBILITY OF DUPLEX STAINLESS STEELS AT THE MICROSCALE

ABSTRACT

In the present paper, grid points coupled with an image analysis method are used to map strain gradients within grains and across interfaces of duplex stainless steels at the micro- and nanoscale under straining conditions (4.5% plastic strain). Highly heterogeneous strain fields are obtained and sites where high strain gradients exist are identified. Local electrochemical measurements are then performed in NaCl-based media within these sites by means of the electrochemical microcell technique and 20 μm microcapillaries in order to propose new mechanical-electrochemical criteria leading to a significant enhancement of anodic and/or cathodic reactions and pitting susceptibility of deformed materials.

Key words : pitting corrosion, duplex stainless steel, microstructure, plastic strain, microprobes

INTRODUCTION

Duplex stainless steels are highly important engineering materials, due to their generally high corrosion resistance and their high strength and toughness. They have a complex microstructure with comparable volume of austenite and ferrite. Due to differences in mechanical properties, a heterogeneous strain distribution is generated in both phases under straining conditions [1] and the presence of these surface strain gradients may affect the physical-chemical properties of the material [2]. Therefore, it is of major importance to quantify surface strains at the microstructure scale. Grid points coupled with an image analysis method appears as powerful tool to map strain gradients within grains and across grain boundaries at the micro- and nanoscale under straining conditions [3].

To provide quantitative criteria for pitting corrosion, it is crucial to analyse the electrochemical response of the material at the same scale. Regarding local electrochemical investigations, the electrochemical microcell technique [4] is extensively used to determine the behaviour and corrosion susceptibility of metallic phases, metallurgical heterogeneities and surface defects in metallic alloys at the microscale.

In the present paper, the two approaches are conducted on the same stainless steel microstructure after plastic deformation and mechanical-electrochemical criteria leading to a significant enhancement of anodic and/or cathodic reactions and pitting susceptibility of deformed materials are proposed.

EXPERIMENTAL

Experiments were performed on a duplex stainless steel (UNS S31803, chemical composition : C: 0.02wt.%; Mn: 1.62%; Ni: 5.45%; Cr: 22.44%; Mo: 2.92%; N: 0.17% and Si: 0.39%). It was hot rolled to obtain 20 mm thick sheets, solution annealed at 1050°C for 15 min and water quenched. Specimens showed a lamellar microstructure with a grain size of about 5 μm in the lamellar direction. In order to increase the grain size, a second heat treatment was carried out consisting of a homogenization treatment at 1300°C for 1 hour, followed by a slow cooling down to 1080°C (formation of the austenite) and a water quenching. The volume fraction of austenite and ferrite was evaluated to 50/50 and the grain size was about 75 μm . The 0.2% yield strength ($R_{p0.2}$) and the ultimate strength (R_m) were 560 and 760 MPa at 25°C, respectively.

Tensile specimens were machined in order to have a cross-section of 2 x 6 mm² and a gauge length of 25 mm. They were mechanically ground using emery papers and polished using diamond pastes (down to 1 μm). The average surface roughness was then evaluated to about 5 nm (calculated on 50 x 50 μm^2 areas). Local electrochemical and mechanical investigations were performed on different sites, as shown in Fig. 1. Specimens were strained up to 4.5% plastic strain at 25°C.

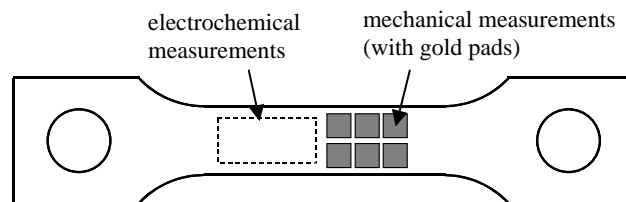


Fig.1. Schematic representation of tensile specimens and areas used for mechanical and electrochemical studies

The local electrochemical measurements were carried out on specimens after unloading in 2M NaCl, pH=3 (solution acidified with HCl) at various temperatures (25°C and 70°C) using the electrochemical microcell technique and 45 μm microcapillaries. A modified high resolution potentiostat was used in order to have a current detection limit of 20 fA (Jaissle 1002T-NC-3). The counter electrode was a platinum wire and the reference electrode was a saturated calomel electrode (SCE).

A conventional process of electron beam lithography was used to deposit grid points. This process is detailed in Ref [3]. The diameter and the height of gold pads were fixed to 70 nm and the distance between pads was set at 730 nm in the two directions. The method used to calculate the strain components can be found in Ref [3].

RESULTS AND DISCUSSION

Pit initiation close to the austenite/ferrite interface

Previous studies at the microscale have shown that highly heterogeneous strain fields exist at the duplex stainless steel surface under straining conditions [3]. It was found that the strain distribution close to the austenite/ferrite interface depends on the mechanical characteristics and morphology of phases. Generally, the strain values measured between two successive gold pads along the loading direction, ε_{11} , was below 10% (slip bands may be observed).

In the absence of large slip bands, ε_{11} can reach values between 25 and 30% in some sites, as shown in Fig. 2. Note that these values are five times higher than the applied strain, of about 4.5%. These strain gradients do not extend over a large distance (only a few micrometers in Regions I and II in Fig. 2) and yield the formation of a rough surface with some surface microcracks.

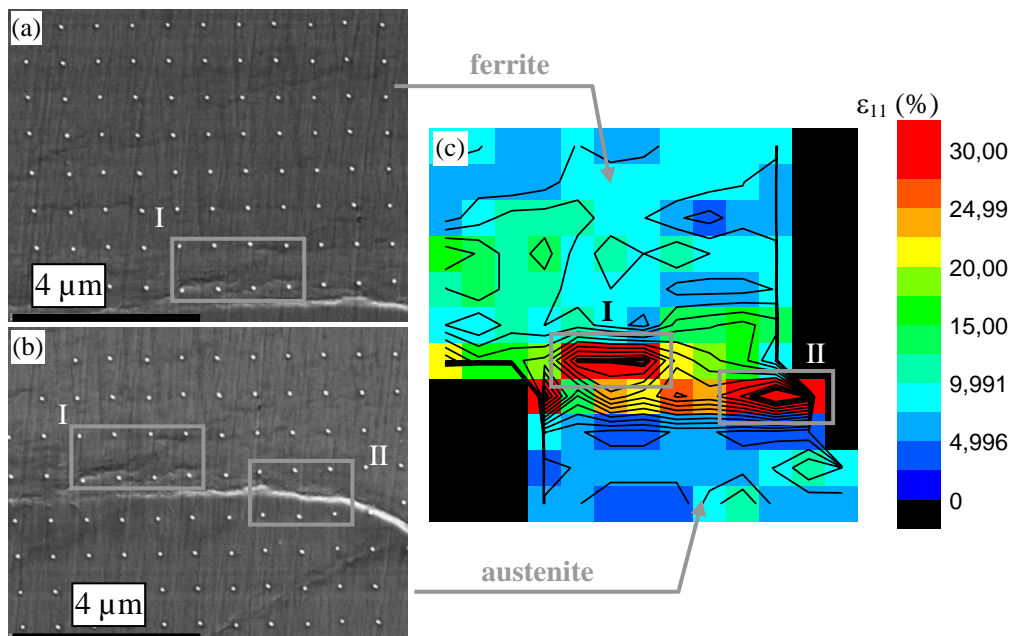


Fig. 2. (a-b) FE-SEM micrographs of the duplex stainless steel surface at the austenite/ferrite interface and the grid points after 4.5% plastic strain. (c) Distribution of the strain along the loading direction, ε_{11} , within the areas shown in (a-b) for a gauge length of 0.73 μm

The current density was plotted versus time at 400 mV/SCE (measurement frequency of 9.1 Hz) in sites containing an interface. At room temperature, the current density calculated in sites defined by $\varepsilon_{11} < 10\%$ reaches the same value as that obtained on the unstrained specimen. In the presence of a rough surface and microcracks (ε_{11} in the range of 25-30%), the current density was higher, indicating that such surface defects affect the electrochemical response of the material. However, no pitting was detected within 900 seconds immersion in 2M NaCl, pH=3, at 25°C. By contrast, stable pitting was observed in some sites defined by $\varepsilon_{11} > 25\%$ after short-time immersion at 70°C, as shown in Fig. 3(b). One may assume that the morphology of microcracks (which may be obtained from AFM images, for instance) is a determining parameter in pit initiation and propagation.

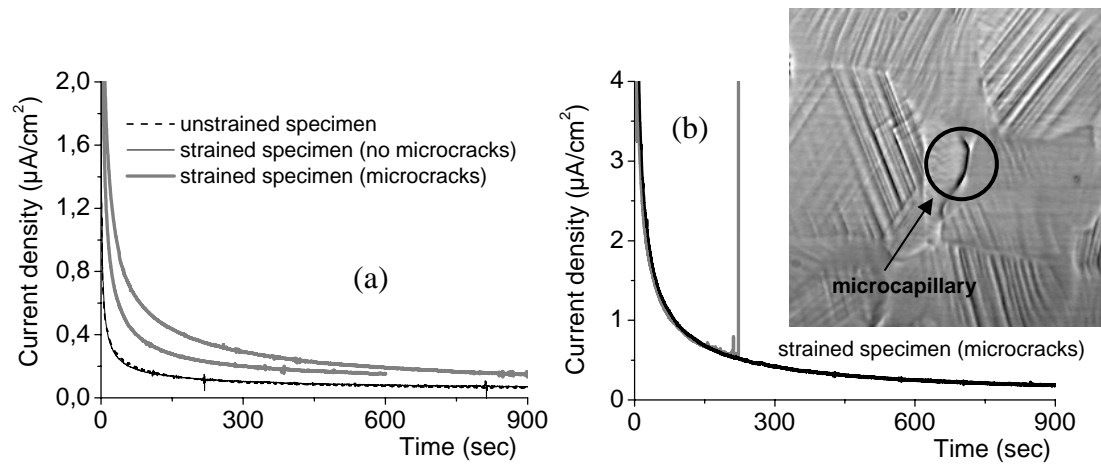


Fig. 3. Evolution of the current density vs. time measured at 400 mV/SCE on sites containing an austenite/ferrite interface. The electrolyte is 2M NaCl, pH=3 at (a) 25°C and (b) 70°C (INSERT – optical micrograph of the site where stable pitting was observed)

Pit initiation in the presence of slip bands

Previous studies at the macroscale have revealed that slip bands are preferential sites for pitting corrosion [5]. The time to pit measured on duplex stainless steels immersed in 0.5M NaCl at 50°C was found to drop significantly in the presence of slip bands. On the basis of these results, the local approach conducted within selected sites containing some specific slip bands will permit to provide criteria leading to pit initiation.

The gauge length was first set at 5.11 μm (the distance between two points of measurement includes seven intervals between pads). Data were averaged and the effects of single slip bands could not be detected. High strain levels (up to about 10%) were generally obtained on grains with a high density of slip bands and the current density measured on these grains at 400 mV/SCE and 25°C was systematically higher than on the polished specimen (Fig. 4(a)). By contrast to the sites close to the interface, metastable and stable pitting was only observed at 650 mV/SCE and 70°C, as shown in Fig. 4(b).

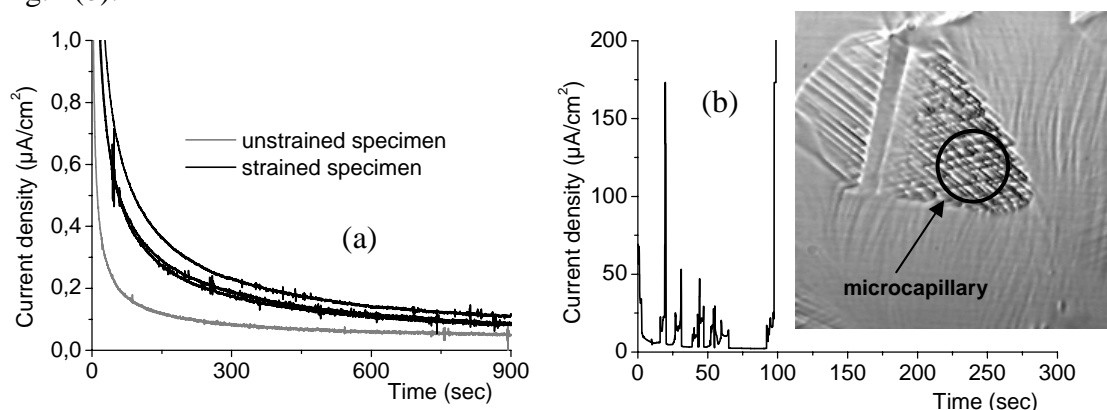


Fig. 4. Evolution of the current density vs. time measured on austenite grains with a high density of slip bands in 2M NaCl, pH=3 : (a) 400 mV/SCE and 25°C; (b) 650 mV/SCE and 70°C (INSERT – optical micrograph of the site where stable pitting was observed)

A high dispersion in the values of ε_{11} was obtained on grains with a low density of slip bands (Fig. 5(a)). Some grains were slightly deformed and ε_{11} was less than the applied strain (values between 3% and 4.5%). The current measured in these grains at 400 mV/SCE and 25°C was close to the values obtained on the polished specimen (Fig. 5(b)). In other austenite grains, ε_{11} was found to be significantly above the applied strain (up to 7%), assuming that sliding parallel to the specimen surface occurred. In this case, the current was higher than on the polished surface but no pitting was detected (even at 650 mV/SCE and 70°C).

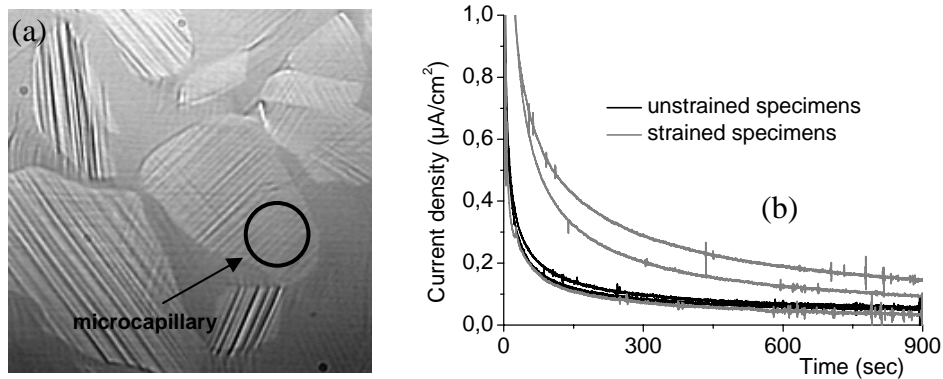


Fig. 5. (a) Optical micrograph of an austenite grain with a low density of slip bands. (b) Evolution of the current density vs. time measured at 400 mV/SCE and 25°C on this type of grains (2M NaCl, pH=3)

Understanding the effects of the presence of slip bands on pitting mechanisms requires information at the sub-microscale. A gauge length of 0.73 μm (the strain is measured between two successive pads) was used to determine the strain at individual slip bands (Fig. 6). The mechanical analysis was performed along the path shown in Fig. 6(a). The evolution of ε_{11} calculated using a gauge length of 0.73 μm revealed the presence of four main peaks defined different strain intensities (peak P1 at 0.73 mm and 8.9%, peak P2 at 3.65 mm and 5.1%, peak P3 at 10.20 mm and 15.7% and peak P4 at 15.30 mm and 7.0% in Fig. 6(b)) and corresponding to the presence of a large slip band at the position of measurement.

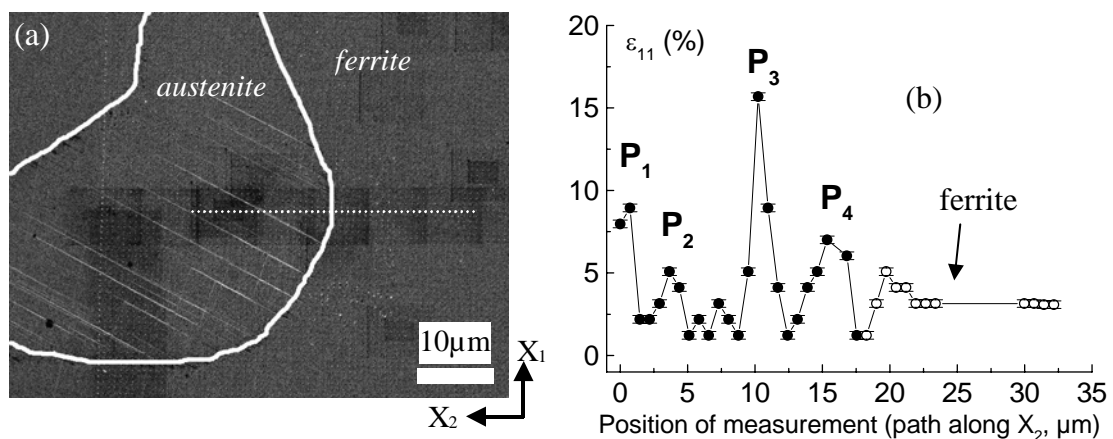


Fig. 6. (a) FE-SEM image of the microstructure where the mechanical analysis was performed along the dotted line. (b) Evolution of ε_{11} along the X_2 -axis calculated for a gauge length of 0.73 μm (the mechanical analysis was performed on the micrograph in (a))

Two-dimensional mapping at some slip bands also demonstrates that strain concentrations may be developed at some point defects of slip bands, as shown in sites A and B in Fig. 7 where the strain value is 25% and 20%, respectively. These sites may be good precursor sites for pitting.

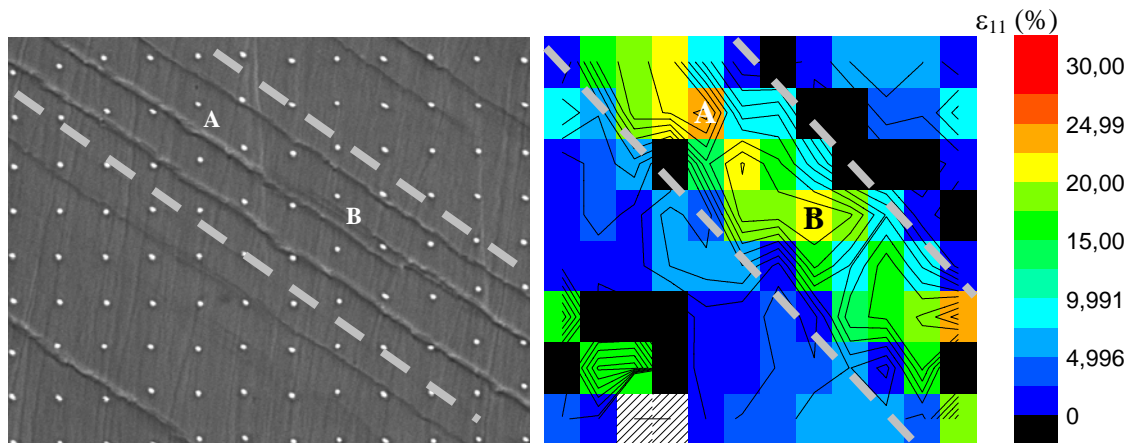


Fig. 7. (a) FE-SEM micrograph of slip bands at the duplex stainless steel surface after 4.5% plastic strain. (b) 2D mapping of the strain along the loading direction, ϵ_{11} , within the area shown in (a) for a gauge length of 0.73 μm

CONCLUSIONS

Grid points coupled with an image analysis method are used to map strain gradients at the surface of duplex stainless steels at the micro- and nanoscale under straining conditions (4.5% plastic strain) and microcells are used to determine the behaviour of sites containing slip bands or microcracks. Stable pits initiated at microcracks in the austenite in 2M NaCl, pH=3, at 400 mV/SCE and 70°C. On the other hand, stable pits were observed in grains with a high density of slip bands at 650 mV/SCE. When a single slip band system was activated, metastable pits were detected.

REFERENCES

1. Mary N., Vignal V., Oltra R. and Coudreuse L.: Finite-element and XRD methods for the determination of the residual surface stress field and the elastic-plastic behaviour of duplex stainless steels. *Philosophical Magazine* 85 (2005), pp.1227-1242.
2. Vignal V., Mary N., Oltra R. and Peultier J.: A mechanical-electrochemical approach for the determination of precursor sites for pitting corrosion at the microscale. *Journal of the Electrochemical Society*, 153 (2006), pp. B352-B357.
3. Kempf D., Vignal V., Cailletaud G., Oltra R., Weeber J.C. and Finot E.: High spatial resolution strain measurements at the surface of duplex stainless steels. *Philosophical Magazine*, in press.
4. Krawiec H., Vignal V. and Banas J.: Macroscopic and Local Electrochemical Studies of Austempered Ductile Iron in Perchlorate Solutions. *Journal of the Electrochemical Society*, 153 (2006), pp. B231-B237.
5. Vignal V., Mary N., Valot C., Oltra R. and Coudreuse L.: Influence of an elastic deformation on the initiation of pits on duplex stainless steels. *Electrochemical and Solid-State Letters*, 7 (2004), pp. C39-C42.